

Contrast Dose and Radiation Dose Reduction in Abdominal Enhanced Computerized Tomography Scans with Single-phase Dual-energy Spectral Computerized Tomography Mode for Children with Solid Tumors

Tong Yu, Jun Gao, Zhi-Min Liu, Qi-Feng Zhang, Yong Liu, Ling Jiang, Yun Peng
Imaging Center, Beijing Children's Hospital, Capital Medical University, Beijing 100045, China

Abstract

Background: Contrast dose and radiation dose reduction in computerized tomography (CT) scan for adult has been explored successfully, but there have been few studies on the application of low-concentration contrast in pediatric abdominal CT examinations. This was a feasibility study on the use of dual-energy spectral imaging and adaptive statistical iterative reconstruction (ASiR) for the reduction of radiation dose and iodine contrast dose in pediatric abdominal CT patients with solid tumors.

Methods: Forty-five patients with solid tumors who had initial CT (Group B) and follow-up CT (Group A) after chemotherapy were enrolled. The initial diagnostic CT scan (Group B) was performed using the standard two-phase enhanced CT with 320 mgI/ml concentration contrast, and the follow-up scan (Group A) was performed using a single-phase enhanced CT at 45 s after the beginning of the 270 mgI/ml contrast injection using spectral mode. Forty percent ASiR was used for the images in Group B and monochromatic images with energy levels ≥ 60 keV in Group A. In addition, filtered back-projection (FBP) reconstruction was used for monochromatic images < 60 keV in Group A. The total radiation dose, total iodine load, contrast injection speed, and maximum injection pressure were compared between the two groups. The 40 keV and 60 keV spectral CT images of Group A were compared with the images of Group B to evaluate overall image quality.

Results: The total radiation dose, total iodine load, injection speed, and maximum injection pressure for Group A were decreased by 19%, 15%, 34.4%, and 18.3%, respectively. The optimal energy level in spectral CT for displaying the abdominal vessels was 40 keV. At this level, the CT values in the abdominal aorta and its three branches, the portal vein and its two branches, and the inferior vena cava were all greater than 340 Hounsfield unit (HU). The abdominal organs of Groups A and B had similar degrees of absolute and relative enhancement ($t = 0.36$ and -1.716 for liver, -0.153 and -1.546 for pancreas, and 2.427 and 0.866 for renal cortex, all $P > 0.05$). Signal-to-noise ratio of the abdominal organs was significantly lower in Group A than in Group B ($t = -8.11$ for liver, -7.83 for pancreas, and -5.38 for renal cortex, all $P < 0.05$). However, the subjective scores for the 40 keV (FBP) and 60 keV (40% ASiR) spectral CT images determined by two radiologists were all > 3 , indicating clinically acceptable image quality.

Conclusions: Single-phase, dual-energy spectral CT used for children with solid abdominal tumors can reduce contrast dose and radiation dose and can also maintain clinically acceptable image quality.

Key words: Contrast Dose Reduction; Pediatric; Radiation Dose Reduction; Solid Tumors

INTRODUCTION

With the rapid development of hardware and postprocessing techniques, computerized tomography (CT) examination has now become the favorite diagnostic method for many diseases.^[1-6] However, the problems of radiation exposure and adverse reactions to contrast are still a concern of the public.^[7-11] More and more studies have proven that the primary forms of damage from radiation are cell malignant

Address for correspondence: Dr. Yun Peng,
Imaging Center, Beijing Children's Hospital, Capital Medical University,
Beijing 100045, China
E-Mail: ppengyun@hotmail.com

This is an open access article distributed under the terms of the Creative Commons Attribution-NonCommercial-ShareAlike 3.0 License, which allows others to remix, tweak, and build upon the work non-commercially, as long as the author is credited and the new creations are licensed under the identical terms.

For reprints contact: reprints@medknow.com

© 2017 Chinese Medical Journal | Produced by Wolters Kluwer - Medknow

Access this article online

Quick Response Code:



Website:
www.cmj.org

DOI:
10.4103/0366-6999.202731

Received: 17-10-2016 **Edited by:** Li-Min Chen
How to cite this article: Yu T, Gao J, Liu ZM, Zhang QF, Liu Y, Jiang L, Peng Y. Contrast Dose and Radiation Dose Reduction in Abdominal Enhanced Computerized Tomography Scans with Single-phase Dual-energy Spectral Computerized Tomography Mode for Children with Solid Tumors. Chin Med J 2017;130:823-31.

transformation and genetic damage.^[7,8] Therefore, increasing the dose of radiation exposure can greatly increase the risk of all types of diseases from malignant tumors to gene damage. Children have higher radiation sensitivity and longer average life expectancy than adults,^[10,11] so it is more important to explore and promote clinical and scientific research regarding low-dose CT scanning protocols for children.^[11-13] Adverse contrast reaction is another problem that should not be ignored in CT examination. The value of CT largely depends on the use of contrast.^[14,15] High-iodine-concentration contrast has higher osmotic pressure and viscosity, which can cause a variety of adverse reactions, such as changes in vascular endothelial cell morphology and function, nausea, vomiting, redness, fever, extravasation, and pain and subcutaneous tissue damage at the injection site.^[15,16] Studies have shown that contrast-related adverse reactions are significantly correlated with the concentration of the contrast, dose of the contrast, and injection pressure.^[16-18] CT contrast can also induce contrast nephropathy, a very serious complication. A survey showed that contrast are the third most frequent causes of iatrogenic acute renal failure.^[19,20] High-risk populations prone to adverse reactions to contrast include infants and young children.^[21] For these high-risk populations, we should reduce the concentration of the contrast and slow down the contrast injection speed to prevent adverse reactions^[16,19-24] while maintaining image quality.

Dual-energy spectral CT simultaneously acquired the raw data per location at two different energies (80 and 140 kVp) in a single 360° gantry rotation. With the use of dedicated analysis tools on an advanced workstation, CT value versus kiloelectron-volt curves can be generated by plotting the attenuation values (in Hounsfield units) of a material at every monochromatic energy from 40 to 140 keV. The resultant is called spectral attenuation curve.^[25] Iodine has markedly increased attenuation at lower energies and decreased attenuation at higher energies.^[22] In conventional CT, better CT angiography (CTA) image was acquired by increasing the concentration or the dose of the contrast, or the use of a lower scanning voltage. However, in dual-energy spectral CT, better CTA image can be acquired by adjusting kiloelectron-volt on workstation; low kiloelectron-volt photon energies can significantly improve the attenuation values of blood vessels, even if the intravascular contrast concentration is low.

The needs to reduce both the radiation dose and contrast dose to children in CT are urgent because of their sensitivity to radiation damage and the side effects of contrast.^[10,11,21] However, there have been few studies on the application of low-concentration contrast in pediatric abdominal CT examinations. This was a feasibility study of the use of dual-energy spectral imaging and adaptive statistical iterative reconstruction (ASiR)^[26] to reduce the radiation and iodine contrast doses in pediatric abdominal CT patients with solid tumors.

METHODS

Patient selection

This study involved patients with solid tumors who underwent initial tumor diagnostic imaging with conventional enhanced CT mode and follow-up evaluation with dual-energy spectral CT mode after chemotherapy. This study was approved by the ethics committee of our hospital. The parents of all pediatric patients signed informed consent to authorize the use of dual-energy spectral CT data and previous relevant enhanced CT images.

There were 45 patients enrolled in our study, and the average age was 3.15 ± 1.03 years (2–6 years), with male/female ratio of 26/19. There were 16 patients with neuroblastoma, 12 with lymphoma, 6 with hepatoblastoma, 4 with rhabdomyosarcoma, and 7 with nephroblastoma. These patients had undergone conventional abdominal enhanced CT scans from September 25, 2014 to March 1, 2015 for diagnosing solid tumors (Group B). Follow-up abdominal enhanced dual-energy spectral CT scans (Group A) were performed from March 1, 2015 to September 30, 2015, after the first course of chemotherapy for pediatric solid tumors to evaluate the volume changes of tumor foci [Table 1].

Computerized tomography scan parameters

Abdominal CT scans were performed on a Discovery CT750 HD (GE Healthcare, Wisconsin, USA). Ten percent chloral hydrate (0.5 ml/kg) was administered half an hour before the CT scan for sedation if needed. The total dose was <10 ml.

A single enhanced phase CT scan was carried out for patients in Group A using dual-energy spectral CT imaging mode with the lowest dose dual-energy spectral CT protocol of 260 mA tube current and a 1.375 helical pitch. The single enhanced phase was performed at 45 s after the beginning of contrast

Table 1: The characteristics of all patients

Characteristics	Results
Number of patients	45
Male/female (<i>n</i>)	26/19
Age (years), mean \pm SD (range)	3.15 ± 1.03 (2–6)
Type of disease (<i>n</i>)	
Neuroblastoma cells	16
Lymphoma	12
Hepatoblastoma	6
Rhabdomyosarcoma	4
Nephroblastoma	7
Weight (kg), mean \pm SD	
Group A (<i>n</i> = 45)	16.04 ± 4.12
Group B (<i>n</i> = 45)	16.76 ± 4.58
Height (cm), mean \pm SD	
Group A (<i>n</i> = 45)	104.90 ± 16.53
Group B (<i>n</i> = 45)	104.87 ± 16.64
BMI (kg/m ²), mean \pm SD	
Group A (<i>n</i> = 45)	14.61 ± 1.94
Group B (<i>n</i> = 45)	15.24 ± 2.05

BMI: Body mass index; SD: Standard deviation.

injection. Monochromatic image sets with photon energies ranging from 40 keV to 140 keV were reconstructed from the single, dual-energy spectral CT scan. Spectral CT images with photon energy levels ranging from 40 keV to 59 keV were reconstructed using the filtered back-projection (FBP) reconstruction algorithm (due to the lack of an iterative reconstruction option for this energy range for the software on our CT system). In addition, the spectral CT images at 60 keV were reconstructed with a 40% ASiR algorithm.

The patients in Group B were scanned using the conventional three-phase scan protocol with an unenhanced phase plus two contrast-enhanced phases. All scans in Group B used the automatic tube current modulation technique and a helical pitch of 1.375 to achieve an image noise index of 9. Tube voltage varied based on the scan phase: 120 kVp for the unenhanced phase; 80 kVp for the arterial phase (AP), with scan beginning 2–3 s after the end of contrast injection; and 120 kVp for the venous phase (VP), with scan beginning 45 s after the beginning of contrast injection. The images in Group B were reconstructed with the 40% ASiR algorithm. The scan ranges were the same for the two groups.

Contrast injection scheme

The contrast was intravenously injected at high speed with a high-pressure syringe at a dose of 1.4 ml/kg for patients with 10–20 kg body weights and 1.2 ml/kg for patients with 20–50 kg body weights. Group A and Group B received 270 mgI/ml and 320 mgI/ml iodixanol contrast, respectively. The injection finished in <15 s in Group B and in <25 s in Group A. The injection rate and the maximum pressure during injection were recorded.

Data measurement and image evaluation

Vessel enhancement evaluation for arteries, portal veins, and inferior vena cava

Vessel enhancement evaluation was carried out using the 40 keV monochromatic images with FBP reconstruction in the dual-energy spectral CT group (Group A) and the conventional CT images with 40% ASiR reconstruction in Group B on an advanced workstation. A region of interest (ROI) of two-thirds of the diameter of the vessel (30–50 mm²) was chosen on the arteries, portal vein, and inferior vena cava (at the site where the renal vein joins the vena cava and at the second hepatic portal vein level) to measure the CT number. Another ROI (50 mm²) was chosen on the erector spinae on the same image to measure the CT number and standard deviation (SD). For the arteries, the abdominal aorta was considered the first-level artery; the renal artery, celiac artery, and superior mesenteric were the second-level arteries; and the splenic artery and hepatic artery were the third-level arteries. For the portal veins, the portal vein trunk was considered the first portal vein level; the right and left branches of the portal vein were the second portal vein level.^[23]

Optimal kiloelectron-volt value

From the vessel enhancement measurement, a contrast-to-noise ratio (CNR) can be calculated: $CNR = (CT[\text{vessel}] - CT[\text{erector spinae}]) / SD(\text{erector spinae})$. The CNR calculation for

dual-energy spectral CT was propagated to the entire photon energy range from 40 keV to 140 keV automatically by the gemstone spectral imaging (GSI) software on AW4.5 (GE Medical Systems, Milwaukee, WI, USA). From the CNR curve covering the entire energy spectrum, one can then select the optimal energy level for achieving the highest CNR value.

Subjective evaluation of image quality in terms of vascular enhancement

The optimal energy spectral CT images were preselected and then presented to reviewers. Subjective evaluations of image quality in terms of vessel enhancement were performed for the axial, coronal, and sagittal images for both the optimal energy level dual-energy spectral CT images reconstructed with the FBP algorithm and for the conventional images reconstructed with 40% ASiR. Two senior radiologists subjectively and blindly evaluated the quality of the images in terms of vascular enhancement using a 4-grade scale, and scores ≥ 3 were considered diagnostic quality. The evaluation standards for abdominal aortic imaging were as follows:

- Score 4: Full diagnostic image quality: The edge of the abdominal aorta was sharp and smooth, with minimal noise. The CT values of the first-, second-, and third-level arteries were more than 300 Hounsfield unit (HU), and the fourth-level artery could be displayed clearly
- Score 3: Diagnostic image quality: The edge of the abdominal aorta was clear, and the artery walls were relatively smooth, with some noise. The CT values of the first-, second-, and third-level arteries were 250–300 HU. The fourth-level artery could be displayed well
- Score 2: Questionable for diagnosis: The edge of the abdominal aorta was not very clear, and the artery walls were rough, with high noise. The CT values of the first-, second-, and third-level arteries were 200–250 HU. The fourth arterial vessel level could not be distinguished
- Score 1: Nondiagnostic: The CT values of the abdominal aorta were <200 HU. The fourth arterial vessel level could not be identified.

The evaluation standards for the portal vein and inferior vena cava were as follows:

- Score 4: Full diagnostic image quality: The portal veins or inferior vena cava at the second hepatic portal area and the hepatic veins (up to third level) could be imaged clearly, with sharp edge and minimal noise. The CT values of the third-level vessel were greater than 200 HU, with high contrast to the liver parenchyma or surrounding tissue
- Score 3: Diagnostic image quality: The portal veins or inferior vena cava (up to third level) could be imaged well, but the walls of the vessels were slightly rough, with some noise. The CT values of the third-level vessels were 150–200 HU, with good contrast to the liver parenchyma or surrounding tissue
- Score 2: Questionable for diagnosis: The portal veins or inferior vena cava had poor contrast to the liver parenchyma or surrounding tissue, and the vessel walls were very rough, with high noise. The CT values of the vessels were <150 HU

- Score 1: Nondiagnostic: The portal veins or inferior vena cava could not be distinguished.

Abdominal parenchyma evaluation

Enhancement and image noise for the abdominal organs were measured on the 60 keV spectral CT images and conventional CT images, both reconstructed with 40% ASiR.

Objective evaluation

A 20-mm² ROI was chosen on the muscle by the spine, left lobe of the liver, head of the pancreas, and renal cortex, avoiding obvious uneven density areas and large vessel branches, to measure the CT number and its SD. The signal-to-noise ratios (SNRs) for these organs were calculated as follows: $SNR = CT(\text{organ})/SD(\text{organ})$. The ratio of the signal of the abdominal organs to that of the muscle was defined as the relative enhancement for the parenchyma and was calculated.

Subjective evaluation

Two senior radiologists evaluated the image quality for the abdominal parenchyma for the axial, coronal, and sagittal 60 keV spectral images with 40% ASiR using a 5-grade scale, which mainly included the following aspects: the hepatic parenchyma and hepatic vasculature; gallbladder wall; spleen parenchyma; pancreatic contour; renal and proximal urethra; blood vessels, such as the celiac origin, mesenteric artery, and renal vasculature; and solid tumor contour and details within the tumor, such as uneven enhancement, vessel shapes, and blood supply. Scores ≥ 3 were considered diagnostic quality.

The evaluation criteria for abdominal organ enhancement, uniformity, and tumor foci were as follows:

- Score 5: Full diagnostic image quality with minimal noise, very clearly displayed structures and lesion detail. Lesions had very clear boundaries and very good contrast to adjacent tissue. The enhancement mode could be clearly determined
- Score 4: Full diagnostic image quality with some noise, well displayed structures and lesion detail. Lesions had clear boundaries and good contrast to adjacent tissue. The enhancement mode could be clearly determined
- Score 3: Diagnostic image quality with moderate noise. Organ structures and lesion details could still be displayed, with some blurred boundaries. The enhancement mode could be determined
- Score 2: Poor image quality with high noise and unclear structure displays, in which lesions could be partly distinguished, and the enhancement mode could not be confidently determined. The image could not be used for diagnosis
- Score 1: Very poor image quality with severe noise and unclear structure displays, in which lesions could not be distinguished, and the enhancement mode could not be determined. The image could not be used for diagnosis.

Contrast dose and radiation dose

The contrast dose and radiation dose (volumetric CT dose index [CTDI_{vol}]) of the two groups were recorded and compared.

Statistical analysis

In this study, a before-and-after analysis of image quality for the same group of children with solid tumors was conducted. Therefore, the paired *t*-test was used for the quantitative measurements, assuming distribution of the before-after differences follows a Gaussian distribution. The boxplot and column bar graphs were plotted to present detail information. The qualitative image quality scores were compared using the Wilcoxon signed-rank test, and the consistency of subjective scores between the two radiologists was evaluated using the kappa test ($\kappa \leq 0.2$ for poor consistency, $0.2 < \kappa \leq 0.4$ for low consistency, $0.4 < \kappa \leq 0.6$ for medium consistency, $0.6 < \kappa \leq 0.8$ for good consistency, and $0.8 < \kappa \leq 1$ for high consistency). All statistical analyses were performed using SPSS version 13.0 (SPSS Inc., Chicago, IL, USA) and a $P < 0.05$ was considered statistically significant.

RESULTS

Contrast injection parameters and radiation doses

The contrast injection parameters and radiation doses for the two groups are listed in Table 2 and Figure 1. Compared with Group B, the contrast concentration and total iodine load were reduced by 15% and 15.8% in Group A, respectively, whereas the injection speed and the maximum pressure during contrast injection were also reduced by 34.4% and 18.3%, respectively. The differences were significant. With the use of single-phase enhanced scanning, dual-energy spectral CT reduced the total radiation dose by 19%, which was also statistically significant.

Optimal kiloelectron-volt selection in dual-energy spectral imaging

CNR curves as a function of photon energy were generated by GSI viewer software. The CNR curves for the abdominal aorta, portal vein, and vena cava had two peaks [Figure 2], with the highest one at 40 keV and the second highest one at 57–65 keV (62.61 ± 1.28 keV). Therefore, the optimal energy levels for the study group were selected at 40 keV and 60 keV, with the 40 keV images being chosen to evaluate the vascular enhancement and 60 keV images to evaluate the abdominal organs where the ASiR technique could be applied for dual-energy spectral CT imaging through our scanner.

Vascular enhancement

The vascular enhancement numbers for the abdominal arteries, portal veins, and inferior vena cava are listed in Table 3. The images in Group A were monochromatic images at 40 keV, and the images in Group B were from conventional contrast-enhanced images in the AP for the abdominal arteries and in the VP for the portal veins and inferior vena cava. The results showed that the abdominal aorta and its second- and third-level branches, the portal vein and its first-level branches, and the inferior vena cava had sufficient enhancement on the 40 keV spectral images for adequate vessel display (higher than 200 HU

Table 2: Parameters of contrast injection and radiation dose

Parameters	Group A (n = 45)	Group B (n = 45)	t	P
Contrast concentration (mg/ml)	270	320		
Injection volume (ml)	22.24 ± 4.10	22.29 ± 3.98	-0.29	0.77
Total iodine load (g)	6.01 ± 1.11	7.13 ± 1.27	-22.14	<0.001
Injection speed (ml/s)	0.97 ± 0.27	1.70 ± 0.62	-13.61	<0.001
Maximum pressure (PSI)	64.80 ± 17.42	79.24 ± 17.20	-40.72	<0.001
CTDIvol (mGy)	4.71 ± 0.00	5.81 ± 1.20	6.18	<0.001

PSI: Pounds per square inch, 1 PSI=6.895 kPa. CTDIvol: Volumetric CT dose index; CT: Computed tomography.

Table 3: Vascular enhancement of all patients (HU)

Items	Group A* (n = 45)	Group B (n = 45)	t	P
Abdominal aorta	409.47 ± 65.63	410.80 ± 30.14	-0.14	0.89
The second-level artery	368.79 ± 63.42	394.33 ± 59.46	-2.76	0.01
The third-level artery	346.74 ± 59.93	366.77 ± 64.62	-2.29	0.03
Portal vein	402.47 ± 60.77	161.00 ± 52.29	26.06	<0.01
Left + right portal vein	391.88 ± 55.44	165.38 ± 55.38	26.48	<0.01
Inferior vena cava	350.60 ± 53.54	156.80 ± 42.26	24.82	<0.01

*40 keV. HU: Hounsfield unit.

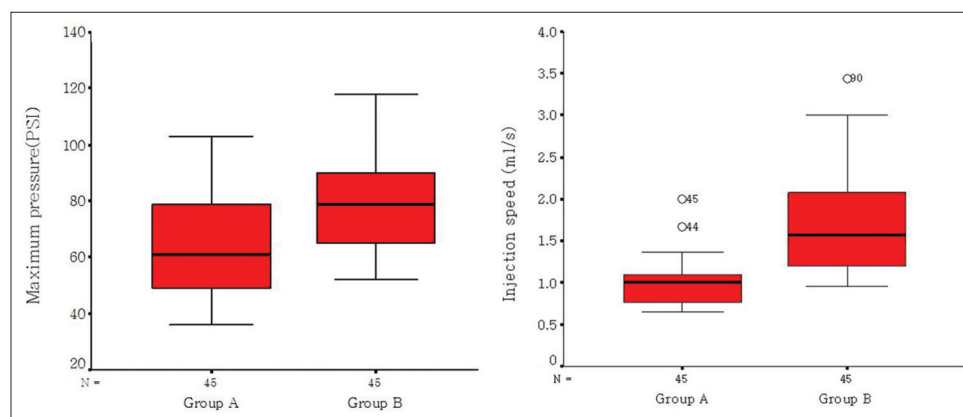


Figure 1: Boxplot of the maximum pressure and injection speed: The left was the boxplot of the maximum pressure of the two groups when contrast injecting (64.80 ± 17.42 and 79.24 ± 17.20 , $t = -40.72$, $P < 0.001$), and the right one was the injection speed when contrast injecting (0.97 ± 0.27 and 1.70 ± 0.62 , $t = -13.61$, $P < 0.001$). PSI: Pounds per square inch (1 PSI=6.895 kPa).

for arteries and higher than 150 HU for veins).^[24] The enhancement in the portal veins and vena cava in the study group (Group A) was significantly higher than that in the control group (Group B) ($P < 0.001$). The CT values in the portal vein, first-level branches of the portal vein, and vena cava in Group A were 2.50, 2.37, and 2.24 times of those in Group B, respectively.

Subjective evaluation of vascular imaging

The subjective evaluation results for the abdominal arteries, portal veins, and vena cava are listed in Table 4. All scores were higher than 3, indicating that all images could be used for diagnosis [Figure 3]. The two readers had excellent agreement on the quality scores ($\kappa = 0.89$).

The results suggested that the 40 keV dual-energy spectral CT images obtained in a single phase provided better imaging quality for the portal and venous vessels than conventional abdominal enhanced CT scans in the individual scan phase, with higher scores (3.48 ± 0.50 vs. 3.21 ± 0.41

for the portal veins and 3.44 ± 0.50 vs. 3.05 ± 0.22 for the inferior vena cava, $P < 0.001$).

Correlations of body mass index and image quality

The average body mass index (BMI) levels of Group A and Group B were 14.61 ± 1.94 kg/m² and 15.24 ± 2.05 kg/m², respectively, with no statistically significant difference. The average BMI of this study was 14.93 ± 2.01 kg/m².

The CT number SD of the muscle was used as the index for image quality. The average SD of Group A was 10.39 ± 2.07 HU. The average SD of Group B was 9.40 ± 2.30 HU. The average BMI and SD of this study had no correlation ($R = -0.031$, $P = 0.769$).

Image quality evaluation for the abdominal organs

Multiplanar reformat images were reconstructed with thin-slice images at 60 keV for dual-energy spectral CT imaging where the ASiR technology could be applied.

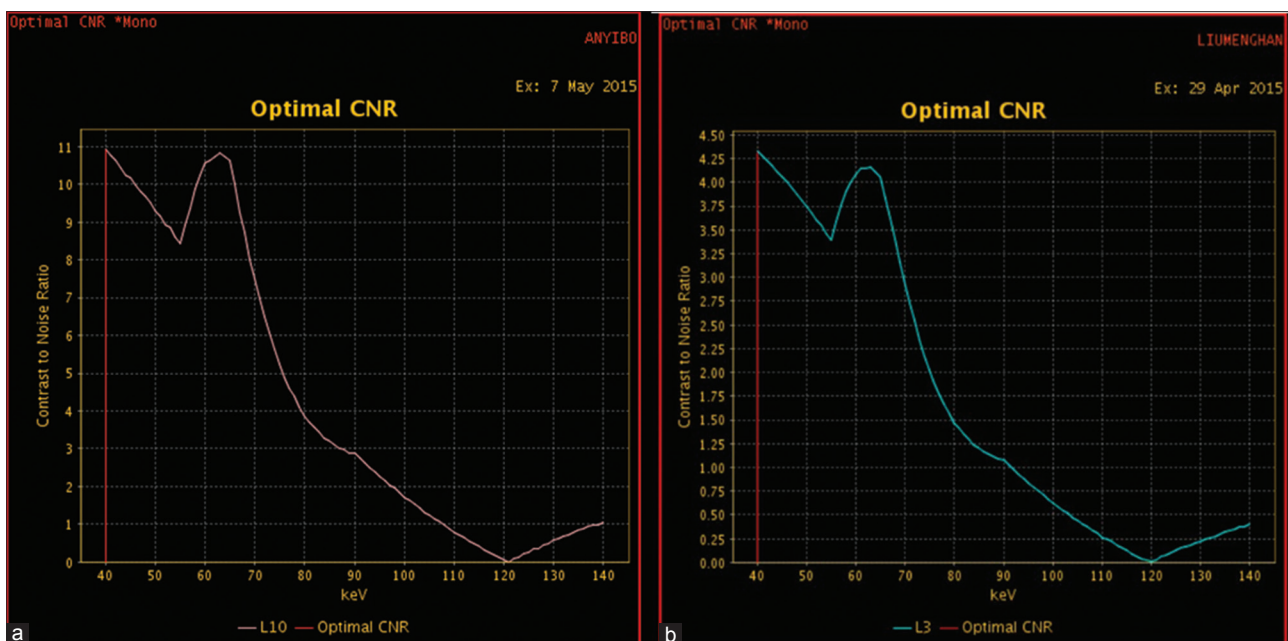


Figure 2: Contrast-to-noise ratio curve of abdominal aorta and inferior vena cava was generated with the gemstone spectral imaging viewer software. Contrast-to-noise ratio curve had two peaks, the highest peak located at 40 keV and the second highest at about 60–63 keV. (a) Abdominal aorta. (b) Inferior vena cava.

The absolute and relative enhancement and image noise for muscle, liver, pancreas, and renal cortex are listed in Table 5. The abdominal organs in Groups A and B had similar degrees of absolute and relative enhancement ($P > 0.05$), while noise was higher in the spectral CT images.

Signal-to-noise ratio and subjective evaluation for the abdominal organs

SNR for the muscle, liver, pancreas, and renal cortex for Group A and Group B were 9.38 ± 1.64 versus 12.81 ± 2.58 , 14.94 ± 2.76 versus 21.22 ± 4.31 , 13.56 ± 2.86 versus 19.45 ± 3.82 , and 21.20 ± 4.32 versus 27.70 ± 6.20 , respectively (all $P < 0.001$).

The subjective evaluation scores for the 60 keV spectral CT images with 40% ASiR of the abdominal organs determined by the two radiologists were all ≥ 3 : 3.69 ± 0.60 for Dr. A and 3.78 ± 0.64 for Dr. B, indicating clinically acceptable images. The agreement between the two observers was good, with $\kappa = 0.75$.

DISCUSSION

In this study, we evaluated the use of a new contrast injection scheme combined with a unique single-phase, dual-energy spectral CT imaging mode for pediatric patients with solid abdominal tumors to reduce both contrast dose and radiation dose. Because the uncertainty in the enhancement of abdominal organs with low-concentration contrast in pediatric abdominal CT images may lead to radiological diagnosis failure, for the initial study, we selected pediatric patients with solid tumors who were undergoing chemotherapy and had undergone enhanced

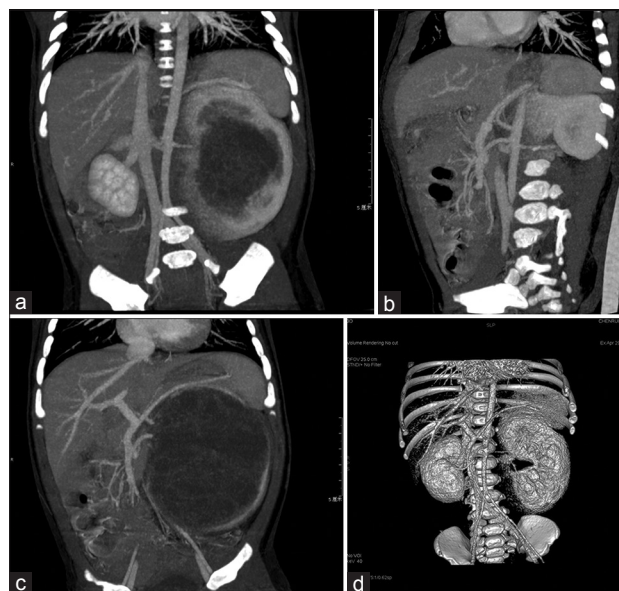


Figure 3: The computerized tomography images of a 1-year-old boy. Left renal cystic partially differentiated nephroblastoma. Thin-slice images of 40 keV were reconstructed. The aorta, portal vein, vena cava, and their main branches are clearly shown on multiplanar reconstructed images of the 40 keV sequence. (a) Coronal image showed that the density of the inferior vena cava and bilateral renal veins was uniform, the edge was clear, and the vessel wall was slightly rough. (b) Oblique sagittal image showed that the density of the 2–3-level branches of aorta was uniform, the edge was clear, and the vessel wall was slightly rough. (c) Coronal images showed that the density of portal vein and its branches were uniform, the edge was clear, and the vessel wall was slightly rough. The portal vein branches in the liver displayed clearly. (d) Volume reconstructing image showed that the edge of aorta, portal vein, inferior vena cava, and its main branches were clear, and the vessel wall was slightly rough.

abdominal CT with a conventional protocol for tumor diagnosis. The primary purpose of the second CT scan was to evaluate the volume changes of the tumor and lymph nodes after chemotherapy. Our results indicated that using a lower concentration contrast and slower contrast injection speed, we could reduce the total contrast dose by 15% with improved patient comfort; using the low-energy monochromatic images in a single-phase, dual-energy spectral CT, we could overcome the adverse effect of reduced contrast dose to obtain satisfactory enhancement in arteries, veins, and various organs while reducing radiation dose by 19%, compared with conventional scan protocols.

The use of contrast in CT scanning can clearly show the contour, shape, and distribution patterns of blood vessels of organs and lesions and increase the diagnostic value of CT, especially for vascular disease.^[14,15] However, the osmotic pressure, viscosity, and high speed of contrast injection can not only make the patient uncomfortable but also induce vascular damage, which can even lead to contrast-related nephropathy.^[16-18,27-32] Newborns, infants, and young children are the high-risk groups for contrast-related adverse reactions.^[21,32-34] Reducing the dose of contrast and the injection speed can effectively prevent such adverse reactions.^[16,19,35,36] The contrast injection speed is uncertain for children, usually determined by nurses according to the child's vascular and sedation conditions, although it is usually fixed in adult abdominal enhanced CT scanning.^[34-36]

In our study, we applied a new contrast injection scheme: reducing both the concentration of contrast and injection speed for contrast dose reduction and patient comfort. Low-concentration contrast (270 mgI/ml) was used in the study group (Group A). The injection speed in Group A was also reduced from the 0.9 to 3.5 ml/s (1.70 ± 0.62 ml/s on average) in the conventional protocol (Group B) to 0.5–1.7 ml/s (0.97 ± 0.27 ml/s on average) based on blood vessel and sedation conditions. The combination of lower contrast concentration and slower injection speed in Group A effectively reduced the total contrast dose to mitigate the chemical damage from the contrast. This contrast scheme also effectively reduced the intravascular pressure (from 79.24 ± 17.20 PSI in Group B to 64.80 ± 17.42 PSI in Group A, $P < 0.001$; 1 PSI=6.895 kPa). Lower injection speed and intravascular pressure can make young children more comfortable and calm, which is important to ensure image quality in the AP.^[36] Immediately, high intravascular pressure caused by rapid intraarterial injection can induce vascular spasms, extravasation. It will bring children limb jitters, body movement, needle abscission, and subcutaneous tissue damage, even waking the child during the injection, which can lead to CT scan failure. Hence, the contrast injection scheme in our study can not only reduce the adverse effects of the contrast in enhanced CT but also improve the success rate of pediatric CT scanning.

The inevitable side effect of reducing contrast dose is the reduction of attenuation in vessels and organs. To overcome this adverse effect, we used the dual-energy spectral CT imaging mode, especially the low-energy monochromatic images for patients in Group A. Dual-energy spectral CT provides images in the energy ranges of 40–140 keV through analysis of two groups of data from 80 kVp to 140 kVp obtained with fast kVp switching.^[27,28] Based on the theory that low-energy X-rays can improve the contrast between high-density and low-density objects, some scholars have attempted enhanced CT diagnosis with low energy,^[28-31] and others have combined

Table 4: Subjective evaluation of vascular imaging, mean \pm SD

Items	Group A* (n = 45)	Group B (n = 45)	t	P
Arteries	3.31 \pm 0.47	3.69 \pm 0.47	-5.09	<0.001
Portal veins	3.48 \pm 0.50	3.21 \pm 0.41	3.61	<0.001
Inferior vena cava	3.44 \pm 0.50	3.05 \pm 0.22	6.36	<0.001

*40 keV. SD: Standard deviation.

Table 5: Enhancement and its uniformity of abdominal organs (HU)

Organ	Group A* (n = 45)	Group B (n = 45)	t	P
Muscle				
Enhancement	68.90 \pm 5.87	65.91 \pm 6.60	2.78	0.065
Uniformity	10.64 \pm 2.06	8.10 \pm 1.66	6.52	<0.001
Liver				
Enhancement	109.96 \pm 12.73	109.02 \pm 11.31	0.36	0.722
Relative enhancement	1.60 \pm 0.17	1.67 \pm 0.24	-1.72	0.093
Uniformity	11.29 \pm 2.08	8.73 \pm 1.31	7.41	<0.001
Pancreas				
Enhancement	99.64 \pm 15.06	100.11 \pm 9.41	-0.15	0.879
Relative enhancement	1.53 \pm 0.22	1.45 \pm 0.24	-1.55	0.129
Uniformity	12.03 \pm 2.36	9.02 \pm 1.64	6.55	<0.001
Renal cortex				
Enhancement	156.11 \pm 24.10	143.22 \pm 24.83	2.43	0.019
Relative enhancement	2.27 \pm 0.33	2.20 \pm 0.46	0.87	0.391
Uniformity	11.31 \pm 2.51	9.10 \pm 2.84	3.82	<0.001

*60 keV. HU: Hounsfield unit.

low-energy level images with low-concentration contrast,^[37] especially for the aorta and the liver vascular system. We evaluated the image quality in terms of enhancement in the vessels and organ parenchyma and image noise with the use of spectral CT images in our study. The image quality of enhanced CT scans is mainly determined by the enhancement of blood vessels and organ parenchyma, which is correlated with the weight of the patient, injection speed, and dose of contrast.^[38-40] Other factors affecting image quality include heart rate, kinemia, circulation, and the basal metabolic rate. The image quality of liver blood vessels is closely related to these factors.^[41] The development of children's tissues and organs is not perfect. The patients in Group A all had solid tumors for at least 2 months and had undergone one course of chemotherapy, so their physiological metabolism and liver and kidney function were not stable. In the face of such large individual differences, it is difficult to judge the peak time accurately, even for experienced radiologists. We performed the enhanced phase at 45 s after the beginning of contrast injection in Group A. Low-energy CT images of dual-energy spectral can increase the ratio of iodine to the surrounding tissues and remedy the decrease in the ratio among a variety of tissues caused by low-concentration contrast. A study suggests that if enhancement of the artery reaches 300 HU or more, 95% of vascular VR images can achieve the best level.^[42] In our study, although the data from our study showed that the enhancement of arteries in Group A was statistically lower than that in Group B (409.47 ± 65.63 vs. 410.80 ± 30.14 HU for the abdominal aorta; 368.79 ± 63.42 vs. 394.33 ± 59.46 HU for the second-level artery; and 346.74 ± 59.93 vs. 366.77 ± 64.62 HU for the third-level artery), two senior radiologists determined that 40 keV energy spectral CT images provided adequate enhancement and displayed vessels very well. Therefore, single enhanced phase spectral CT scan mode can provide us with diagnostically acceptable enhanced vessel images. Single enhanced phase spectral CT mode also provided us with high-quality images of the abdominal organs. In this study, we evaluated and compared organ image quality on 60 keV images with conventional CT enhanced VP images with 40% ASiR. There was no significant CT value difference in the muscle, liver, pancreas, or renal cortex, and the relative enhancement of the organs in Group A was higher than that in Group B. Although the objective noise in the 60 keV spectral images was higher than that in Group B, the opinion of the radiologists was that this increase in objective noise did not affect the display of different components in the tumors.

The results of our study also showed that the CT scanning protocol of dual-energy spectral CT with a single enhanced phase does lowered the radiation dose. The radiation dose (CTDI_{vol}) in Group A was approximately 19% lower than that of the conventional protocol with two enhanced phases.

This study had limitations. First, we had a small number of patients because it was a preliminary exploration of the feasibility of the clinical application of low-concentration contrast. Second, the patients in this study had only solid tumors and were in the midst of medical treatment, so the

conclusions of the study should apply only to children with tumors and are not applicable for patients from whom vascular information is needed.

In this study, we carried out a feasibility study combining dual-energy spectral CT mode and low-concentration contrast for pediatric abdominal enhanced CT scans. We concluded that single-phase, dual-energy spectral CT mode can be used to reduce contrast dose and radiation dose while maintaining clinically acceptable image quality for children with solid abdominal tumors.

Acknowledgments

We would like to express our sincere thanks to Dr. Jian-Ying Li for his technical support in editing the manuscript.

Financial support and sponsorship

This study was supported by a grant from the National Science and Technology Major Project of the Ministry of Science and Technology of China and the Application Research of Clinical Characteristics of Beijing (No. Z141107002514005).

Conflicts of interest

There are no conflicts of interest.

REFERENCES

1. Pan X, Siewerdsen J, La Riviere PJ, Kalender WA. Anniversary paper. Development of X-ray computed tomography: The role of medical physics and AAPM from the 1970s to present. *Med Phys* 2008;35:3728-39. doi: 10.1118/1.2952653.
2. Liguori C, Frauenfelder G, Massaroni C, Saccomandi P, Giurazza F, Pitocco F, *et al.* Emerging clinical applications of computed tomography. *Med Devices (Auckl)* 2015;8:265-78. doi: 10.2147/MDER.S70630.
3. Liu PS, Platt JF. CT angiography in the abdomen: A pictorial review and update. *Abdom Imaging* 2014;39:196-214. doi: 10.1007/s00261-013-0035-3.
4. Frush DP. Pediatric abdominal CT angiography. *Pediatr Radiol* 2008;38 Suppl 2:S259-66. doi: 10.1007/s00247-008-0795-z.
5. Hellinger JC, Pena A, Poon M, Chan FP, Epelman M. Pediatric computed tomographic angiography: Imaging the cardiovascular system gently. *Radiol Clin North Am* 2010;48:439-67. doi: 10.1016/j.rcl.2010.03.005.
6. Uyeda JW, Anderson SW, Sakai O, Soto JA. CT angiography in trauma. *Radiol Clin North Am* 2010;48:423-38. doi: 10.1016/j.rcl.2010.02.003.
7. Brenner DJ, Hall EJ. Computed tomography – An increasing source of radiation exposure. *N Engl J Med* 2007;357:2277-84. doi: 10.1056/NEJMr072149.
8. Yoshinaga S, Mabuchi K, Sigurdson AJ, Doody MM, Ron E. Cancer risks among radiologists and radiologic technologists: Review of epidemiologic studies. *Radiology* 2004;233:313-21. doi: 10.1148/radiol.2332031119.
9. Mettler FA Jr., Bhargavan M, Faulkner K, Gilley DB, Gray JE, Ibbott GS, *et al.* Radiologic and nuclear medicine studies in the United States and worldwide: Frequency, radiation dose, and comparison with other radiation sources–1950-2007. *Radiology* 2009;253:520-31. doi: 10.1148/radiol.2532082010.
10. Pearce MS, Salotti JA, Little MP, McHugh K, Lee C, Kim KP, *et al.* Radiation exposure from CT scans in childhood and subsequent risk of leukaemia and brain tumours: A retrospective cohort study. *Lancet* 2012;380:499-505. doi: 10.1016/S0140-6736(12)60815-0.

11. Thrall JH. Radiation exposure in CT scanning and risk: Where are we? *Radiology* 2012;264:325-8. doi: 10.1148/radiol.12121137.
12. Peng Y, Ma DQ, Li JY, Zhang QF, Liu Y, Wang B, *et al*. Feasibility study of automatic tube current modulation in low-dose thoracic imaging for young children with 64-slice spiral CT. *Chin J Radiol* 2008;42:1045-9. doi: 10.3321/j.issn:1005-1201.2008.10.009.
13. Hall EJ. Lessons we have learned from our children: Cancer risks from diagnostic radiology. *Pediatr Radiol* 2002;32:700-6. doi: 10.1007/s00247-002-0774-8.
14. Lusic H, Grinstaff MW. X-ray-computed tomography contrast agents. *Chem Rev* 2013;113:1641-66. doi: 10.1021/cr200358s.
15. Baerlocher MO, Asch M, Myers A. The use of contrast media. *CMAJ* 2010;182:697. doi: 10.1503/cmaj.090118.
16. Andreucci M, Solomon R, Tasanarong A. Side effects of radiographic contrast media: Pathogenesis, risk factors, and prevention. *Biomed Res Int* 2014;2014:741018. doi: 10.1155/2014/741018.
17. McCullough PA, Capasso P. Patient discomfort associated with the use of intra-arterial iodinated contrast media: A meta-analysis of comparative randomized controlled trials. *BMC Med Imaging* 2011;11:12. doi: 10.1186/1471-2342-11-12.
18. Namasivayam S, Kalra MK, Torres WE, Small WC. Adverse reactions to intravenous iodinated contrast media: A primer for radiologists. *Emerg Radiol* 2006;12:210-5. doi: 10.1007/s10140-006-0488-6.
19. Andreucci M, Faga T, Pisani A, Sabbatini M, Michael A. Acute kidney injury by radiographic contrast media: Pathogenesis and prevention. *Biomed Res Int* 2014;2014:362725. doi: 10.1155/2014/362725.
20. Marenzi G, Bartorelli AL. Recent advances in the prevention of radiocontrast-induced nephropathy. *Curr Opin Crit Care* 2004;10:505-9.
21. Schopp JG, Iyer RS, Wang CL, Petscavage JM, Paladin AM, Bush WH, *et al*. Allergic reactions to iodinated contrast media: Premedication considerations for patients at risk. *Emerg Radiol* 2013;20:299-306. doi: 10.1007/s10140-012-1081-9.
22. Silva AC, Morse BG, Hara AK, Paden RG, Hongo N, Pavlicek W. Dual-energy (spectral) CT: Applications in abdominal imaging. *Radiographics* 2011;31:1031-46.
23. Hu D, Yu T, Duan X, Peng Y, Zhai R. Determination of the optimal energy level in spectral CT imaging for displaying abdominal vessels in pediatric patients. *Eur J Radiol* 2014;83:589-94. doi: 10.1016/j.ejrad.2013.10.016.
24. Han ZL, Peng Y. Reasonable use of contrast medium for achieving adequate and consistent vascular enhancement in CT angiography (in Chinese). *Chin J Interv Imaging Ther* 2012;9:59-61.
25. Lin XZ, Shen Y, Chen KM. Spectral CT imaging: Principle, clinical application and research (in Chinese). *Chin J Radiol* 2011;45:798-800. doi: 10.3760/cma.j.issn.1005-1201.2011.08.028.
26. Liu W, Ding X, Kong B, Fan B, Chen L. Reducing the radiation dose with the adaptive statistical iterative reconstruction technique for chest CT in adults: A parameter study. *Chin Med J* 2014;127:1284-8. doi: 10.3760/cma.j.issn.0366-6999.20131479.
27. Matsumoto K, Jinzaki M, Tanami Y, Ueno A, Yamada M, Kuribayashi S. Virtual monochromatic spectral imaging with fast kilovoltage switching: Improved image quality as compared with that obtained with conventional 120-kVp CT. *Radiology* 2011;259:257-62. doi: 10.1148/radiol.111100978.
28. Zhang D, Li X, Liu B. Objective characterization of GE discovery CT750 HD scanner: Gemstone spectral imaging mode. *Med Phys* 2011;38:1178-88. doi: 10.1118/1.3551999.
29. De Cecco CN, Darnell A, Rengo M, Muscogiuri G, Bellini D, Ayuso C, *et al*. Dual-energy CT: Oncologic applications. *AJR Am J Roentgenol* 2012;199 5 Suppl:S98-105. doi: 10.2214/AJR.12.9207.
30. Zhao LQ, He W, Li JY, Chen JH, Wang KY, Tan L. Improving image quality in portal venography with spectral CT imaging. *Eur J Radiol* 2012;81:1677-81. doi: 10.1016/j.ejrad.2011.02.063.
31. Lv P, Lin XZ, Li J, Li W, Chen K. Differentiation of small hepatic hemangioma from small hepatocellular carcinoma: Recently introduced spectral CT method. *Radiology* 2011;259:720-9. doi: 10.1148/radiol.11101425.
32. Callahan MJ, Poznauskis L, Zurakowski D, Taylor GA. Nonionic iodinated intravenous contrast material-related reactions: Incidence in large urban children's hospital – Retrospective analysis of data in 12,494 patients. *Radiology* 2009;250:674-81. doi: 10.1148/radiol.2503071577.
33. Dillman JR, Strouse PJ, Ellis JH, Cohan RH, Jan SC. Incidence and severity of acute allergic-like reactions to i.v. nonionic iodinated contrast material in children. *AJR Am J Roentgenol* 2007;188:1643-7. doi: 10.2214/AJR.06.1328.
34. Wiklund LM, Brodin I, Sjöholm K. Nonionic contrast media in pediatric CT. A comparative study of intravenous use of iopentol and iohexol. *Acta Radiol* 1994;35:186-90.
35. Jacobs JE, Birnbaum BA, Langlotz CP. Contrast media reactions and extravasation: Relationship to intravenous injection rates. *Radiology* 1998;209:411-6. doi: 10.1148/radiology.209.2.9807567.
36. Cohen MD, Herman E, Herron D, White SJ, Smith JA. Comparison of intravenous contrast agents for CT studies in children. *Acta Radiol* 1992;33:592-5.
37. Zhu Z, Zhao XM, Zhao YF, Wang XY, Zhou CW. Feasibility study of using gemstone spectral imaging (GSI) and adaptive statistical iterative reconstruction (ASIR) for reducing radiation and iodine contrast dose in abdominal CT patients with high BMI values. *PLoS One* 2015;10:e0129201. doi: 10.1371/journal.pone.0129201.
38. Erturk SM, Ichikawa T, Sou H, Tsukamoto T, Motosugi U, Araki T. Effect of duration of contrast material injection on peak enhancement times and values of the aorta, main portal vein, and liver at dynamic MDCT with the dose of contrast medium tailored to patient weight. *Clin Radiol* 2008;63:263-71. doi: 10.1016/j.crad.2007.02.024.
39. Ichikawa T, Nakajima H, Nanbu A, Hori M, Araki T. Effect of injection rate of contrast material on CT of hepatocellular carcinoma. *AJR Am J Roentgenol* 2006;186:1413-8. doi: 10.2214/AJR.04.0310.
40. Platt JF, Reige KA, Ellis JH. Aortic enhancement during abdominal CT angiography: Correlation with test injections, flow rates, and patient demographics. *AJR Am J Roentgenol* 1999;172:53-6. doi: 10.2214/ajr.172.1.9888738.
41. Lv P, Lin XZ, Chen K, Gao J. Spectral CT in patients with small HCC: Investigation of image quality and diagnostic accuracy. *Eur Radiol* 2012;22:2117-24. doi: 10.1007/s00330-012-2485-3.
42. Yu H, Li HM, Yuan Z. Relating factors on image quality of three-dimensional upper abdominal CT angiography (in Chinese). *Chin Comput Med Imaging* 2009;15:358-61. doi: 10.3969/j.issn.1006-5741.2009.04.013.